Arch Appl Mech (2007) 77: 707–728
DOI 10.1007/s00419-007-0122-4

ORIGINAL

Ping Lou

Finite element analysis for train–track–bridge interaction system

Received: 17 June 2006 / Accepted: 18 January 2007 / Published online: 6 March 2007

Abstract This article deals with the dynamic analysis of train–track–bridge interaction system using the finite element method. In this interaction system, each four-wheelset vehicle in the train is modeled by a mass–spring–damper system with 10 degrees of freedom; the rails and the bridge decks are modeled as a number of Bernoulli–Euler beam elements, while the elasticity and damping properties of the rail bed are represented by continuous springs and dampers. The equation of motion for the interaction system is presented in matrix form with time-dependent coefficients. The correctness of the proposed procedure is illustrated by a comparison with the numerical result from the existing literature. Several numerical examples are chosen to investigate the effect of two types of vehicle models, two types of bridge models and three damping values of bridge on the maximum dynamic responses of train, track and bridges.

Keywords Train–track–bridge interaction · Finite element method · Dynamic response · Moving train · Railway track · Railway bridge

1 Introduction

Research on the interaction between traveling vehicles and guideway systems has been abundant. It is not the purpose herein to make a comprehensive review of all the related works. For readers who are interested in a general view of this subject, the survey paper prepared by Kortuem and Wormley [12] may be consulted. The vibrations caused by the passage of vehicles have become an important consideration in the design of bridges. In particular, Au et al. [1] pointed out that the interaction problem between the moving vehicles and the bridge structures has attracted much attention during the last three decades. Here only some of the relevant literature is mentioned. In most of the previous studies, however, much work such as [2,4,6,9–11,14,16,18,20,22,27, 28,30] completely neglected the effects of the track structure.

Some researchers only partially accounted for the effects of the track structures in the investigation of vehicle–bridge interaction. For example, Wiriyachai et al. [25], Chu et al. [7] and Wang et al. [24], took into account the elastic properties of track structures by computing the combined stiffness of track and bridge structures. Yang and Yau [29] as well as Yau et al. [31] accounted for the ballast stiffness of the track structure by continuously distributed springs while implicitly neglecting the flexural stiffness of the rail. However, the damping properties of the track structures have not been taken into account in their studies. Furthermore, the vibration of the track structures could not be analyzed simultaneously in their models.

Recently, the dynamic response of track structures resting on bridges under the action of moving trains has attracted attention from researchers. Le et al. [13] reported some numerical work and field measurements

P. Lou
School of Civil Engineering and Architecture, Railway Campus, Central South University,
22 Shao-shan-nan Road, Changsha, Hunan 410075, People's Republic of China
E-mail: pinglou@mail.csu.edu.cn
E-mail: pingloucsu@126.com

on ballast mats on high-speed bridges. In their study, the track and the bridge were modeled by conventional Timoshenko beam finite elements. Sleepers and ballast were modeled as lump masses interconnected with spring–damper systems. Spring–damper systems in parallel are also used to model the connection between the rail and sleeper as well as between the ballast and bridge. Cheng et al. [5] presented a bridge–track–vehicle element for investigating the interactions among a moving train, track and bridge. In their paper, the vehicle is modeled as two one-axle mass–spring–damper systems. In order to simulate the interaction between the front and rear wheelsets of a two-wheelset vehicle, Lou [15] presented a vehicle–track–bridge interaction element considering the effect of vehicle pitching. Wu and Yang [26] dealt with the two-dimensional steady-state response and riding comfort of a train moving over a series of simply supported railway bridges, together with the impact response of the rails and bridges. In their study, the dynamic response of the vehicle–rails–bridge interaction system was solved by a condensation technique [23]. Lou and Zeng [19] derived the equations of motion of the vehicle–track–bridge interaction element with two types of vehicle models by means of the principle of a stationary value of total potential energy of dynamic system presented by Zeng [32,33], in which the contact forces between vehicle and rails were regarded as internal forces. In their study, the one vehicle model was modeled as a one-foot mass–spring–damper system having two degrees of freedom, and the other was modeled as a four-wheelset mass–spring–damper system with two-stage suspension system possessing 10 degrees of freedom (DOFs). Recently, Lou [17] compared two types of deflection functions for analysing the responses of the rail and the bridge under static or moving vehicles. One type is the shape functions of a beam element described by the cubic Hermitian interpolation functions in the finite element method, and the other is the deflection of a beam described by the superimposing modes in the modal analysis method. However, in his study, the vehicle was modeled as a two-wheelset mass–spring–damper system with four DOFs, and only a simply supported bridge was analyzed.

The aim of this article is to investigate the dynamic responses of the interaction system consisting of a moving train, track and bridge by using the finite element method. This article can be regarded as an extension of the theory presented in [19] . The enhancements introduced in the current work for the train model (series of four-wheelset vehicles) and the possibility to consider multi-span continuous beams to model bridges (and not only single-span simply supported bridges) permits more-realistic analyses. The parametric studies on the dynamic response of the train–track–bridge system will be carried out in this article for various types of bridges and for different damping values of the bridge. In addition, the effect of various types of vehicle models on the dynamic response of the train–track–bridge system will also be studied.

2 Models of train, track and bridge

Figure 1 shows a train consisting of a series of identical four-wheelset vehicles moving on a track structure resting on a series of multi-span continuous beams to model railway bridges and the two approach embankments. The train comprises N_{v} identical vehicles numbered 1, 2, …, N_{v} from left to right and proceeds with speed v and acceleration a at time t along the longitudinal direction. It is assumed that each wheelset of all vehicles always maintains contact with the rails, that is, the separation between the wheelset and the rails is not considered in this article. Each vehicle in the train is modeled as a mass–spring–damper system consisting of a car body, two bogie frames, four wheelsets and two-stage suspensions. As shown in Fig. 2, the car body is modeled as a rigid body with a mass m_{c} and a moment of inertia J_{c} about the transverse horizontal axis through its center of gravity. Similarly, each bogie frame is considered as a rigid body having a mass m_{t} and a moment of inertia J_{t} about the transverse horizontal axis through its center of gravity. Each wheelset has a mass m_{w}. The spring and shock absorber in the primary suspension for each wheelset are characterized by spring stiffness k_{p} and damping coefficient c_{p}, respectively. Likewise the secondary suspension between car body and each bogie frame is characterized by spring stiffness k_{s} and damping coefficient c_{s}. As the car body is assumed to be rigid, the motion of the jth vehicle may be described by the vertical displacement $y_{\mathrm{c}j}$ and rotation $\theta_{\mathrm{c}j}$ at its center of gravity, where the subscript j denotes the vehicle number. Similarly, the motions of the rear bogie frame of the jth vehicle may be described by the vertical displacement $y_{\mathrm{t}1j}$ and rotation $\theta_{\mathrm{t}1j}$ at its center of gravity; the motions of the front bogie frame of the jth vehicle may be described by the vertical displacement $y_{\mathrm{t}2j}$ and rotation $\theta_{\mathrm{t}2j}$ at its center of gravity. The motion of the four wheelsets from left to right of the jth vehicle may be described by the vertical displacements $y_{\mathrm{w}1j}$, $y_{\mathrm{w}2j}$, $y_{\mathrm{w}3j}$ and $y_{\mathrm{w}4j}$, respectively. Therefore, the total number of DOFs for each vehicle is 10. However, the vertical displacement of each wheelset is constrained by the displacement of the rails. Consequently, the independent DOFs for each vehicle become six. It is assumed that the downward vertical displacements and clockwise direction rotation

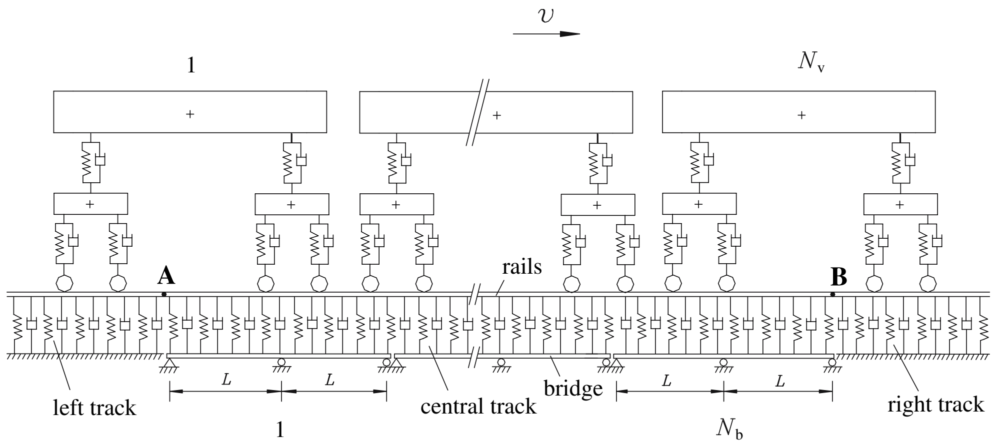

Fig. 1 A typical train–track–bridge interaction system

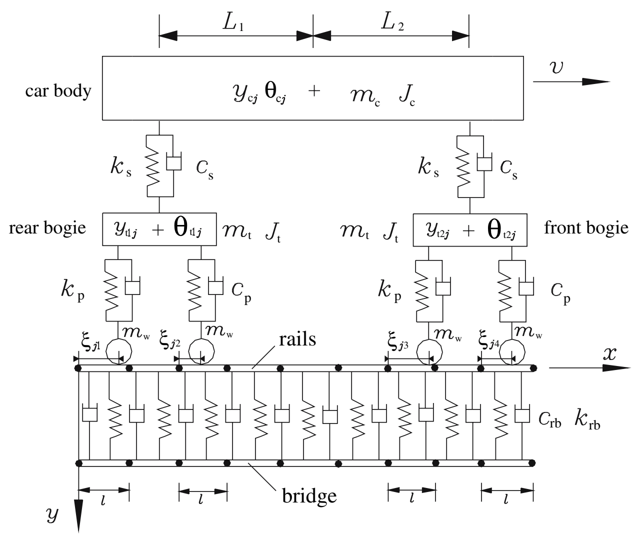

Fig. 2 A vehicle–track–bridge interaction system with the jth vehicle

of vehicle are taken as positive and that they are measured with reference to their respective static equilibrium positions before coming onto the track concerned.

As shown in Fig. 1, the track is divided into three segments, i.e., the left, central and right track segments, to describe conveniently the matrices of the rail–bridge interaction in Sect. 3.6. The left track segment is the track supported on the left embankment, i.e., the track between the left end and point A (point A is above the left end point of the first bridge). Similarly, the right track segment is the track supported on the right embankment, i.e., the track between the right end and point B (point B is above the right end point of the N_bth bridge). The central track segment is the track on the bridges, i.e., the track between points A and B. The two rails are effectively treated as one in the subsequent analysis. The rail is modeled as a linear elastic Bernoulli–Euler beam with finite length, and the bridge decks are modeled as a series of multi-span continuous Bernoulli–Euler beams. The elasticity and damping properties of the rail bed are represented by continuous springs with stiffness k_{rb} and dampers with damping coefficient c_{rb}. On the basis of the finite element method, the rail is divided into a number of beam elements of equal length l, and the bridges are also divided into a series of beam elements of equal length l. It is assumed that the damping of the rail is neglected, and the bridges have linear viscous damping. In addition, neglecting axial deformations of the rail and bridges, each node of the rail and bridges has two DOFs, i.e., vertical displacement and rotation.

It is assumed that the downward deflections of rail and bridge deck are taken as positive and that they are measured with reference to their respective vertical static equilibrium positions. Let $r(x)$ denotes the initial top surface irregularities of rail and is measured with reference to smooth profile of rail, i.e., $r(x) = 0$ if the top surface of rail is smooth. It is considered positive in the downward direction.

3 Equation of motion for train–track–bridge interaction system

By using the principle of a stationary value of total potential energy of a dynamic system presented by Zeng [32,33], one can derive the equation of motion for the train–track–bridge interaction system. For the cubic Hermitian interpolation functions being used for the shape functions of the beam elements of rail and bridge, the equation can be written in submatrix form as

$$\begin{bmatrix} \mathbf{M}_{vv} & \mathbf{0} & \mathbf{0} \\ \mathbf{0} & \mathbf{M}_{rr} & \mathbf{0} \\ \mathbf{0} & \mathbf{0} & \mathbf{M}_{bb} \end{bmatrix} \begin{Bmatrix} \ddot{\mathbf{X}}_v \\ \ddot{\mathbf{X}}_r \\ \ddot{\mathbf{X}}_b \end{Bmatrix} + \begin{bmatrix} \mathbf{C}_{vv} & \mathbf{C}_{vr} & \mathbf{0} \\ \mathbf{C}_{rv} & \mathbf{C}_{rr} & \mathbf{C}_{rb} \\ \mathbf{0} & \mathbf{C}_{br} & \mathbf{C}_{bb} \end{bmatrix} \begin{Bmatrix} \dot{\mathbf{X}}_v \\ \dot{\mathbf{X}}_r \\ \dot{\mathbf{X}}_b \end{Bmatrix} + \begin{bmatrix} \mathbf{K}_{vv} & \mathbf{K}_{vr} & \mathbf{0} \\ \mathbf{K}_{rv} & \mathbf{K}_{rr} & \mathbf{K}_{rb} \\ \mathbf{0} & \mathbf{K}_{br} & \mathbf{K}_{bb} \end{bmatrix} \begin{Bmatrix} \mathbf{X}_v \\ \mathbf{X}_r \\ \mathbf{X}_b \end{Bmatrix} = \begin{Bmatrix} \mathbf{F}_v \\ \mathbf{F}_r \\ \mathbf{F}_b \end{Bmatrix} \tag{1}$$

where the subscripts ‘v’, ‘r’, and ‘b” denote the vehicles, rail, and bridges, respectively. The displacement vectors, the mass, stiffness and damping matrices, and the load vectors of the vehicles, rail, and bridges are explained as follows.

3.1 Displacement vectors

It is assumed that the number of vehicles on the track concerned is N_v. The vehicles displacement vector $\mathbf{X}_v$ with order $(6 \times N_v) \times 1$ can be written

$$\mathbf{X}_v = [\,\mathbf{X}_{v1}\ \mathbf{X}_{v2} \cdots \mathbf{X}_{vN_v}\,]^T \tag{2}$$

where the superscript ‘T’ denotes the transpose of the matrix and $\mathbf{X}_{vj}$ $(j = 1, 2, \ldots, N_v)$ denotes the displacement vector of the jth vehicle. $\mathbf{X}_{vj}$ with order 1×6 can be expressed as

$$\mathbf{X}_{vj} = [\, y_{cj}\ \theta_{cj}\ y_{t1j}\ \theta_{t1j}\ y_{t2j}\ \theta_{t2j}\,] \tag{3}$$

The displacement vector of the rail $\mathbf{X}_r$ with order $N_r \times 1$ can be written

$$\mathbf{X}_r = [\, q_{r1}\ q_{r2} \cdots q_{rN_r}\,]^T \tag{4}$$

where N_r denotes the total number of DOFs of the rail.

The displacement vector $\mathbf{X}_b$ with order $\bar{N}_b \times 1$ for a series of multi-span continuous beams to model the bridges can be written

$$\mathbf{X}_b = [\,\mathbf{X}_{b1}\ \mathbf{X}_{b2} \cdots \mathbf{X}_{bN_b}\,]^T \tag{5}$$

where $\mathbf{X}_{bi}$ $(i = 1, 2, \ldots, N_b)$ denotes the displacement vector of the ith A bridge, N_b the total number of multi-span bridges, as shown in Fig. 1, and $\bar{N}_b$ is the total number of DOFs of all bridges. $\mathbf{X}_{bi}$ with order $1 \times n_{bi}$ and $\bar{N}_b$ can be expressed as

$$\mathbf{X}_{bi} = [\, q_{b1}\ q_{b2} \cdots q_{bn_{bi}}\,] \tag{6}$$

$$\bar{N}_b = \sum_{i=1}^{N_b} n_{bi} \tag{7}$$

where n_{bi} denotes the total number of DOFs of the ith multi-span bridge.

3.2 Matrices for the vehicles

The matrices of the vehicles are marked with the subscript ‘vv’. The mass matrix $\mathbf{M}_{vv}$ of the vehicles, with order $(6 \times N_v) \times (6 \times N_v)$, can be written

$$\mathbf{M}_{vv} = \mathrm{diag}[\,\mathbf{M}_{v1}\ \mathbf{M}_{v2}\ \cdots\ \mathbf{M}_{vN_v}\,] \tag{8}$$

where $\mathbf{M}_{vj}$ with order 6×6 denotes the mass matrix of the jth vehicle and can be expressed as

$$\mathbf{M}_{vj} = \mathrm{diag}[\,m_c\ J_c\ m_t\ J_t\ m_t\ J_t\,] \tag{9}$$

The stiffness matrix $\mathbf{K}_{vv}$ of the vehicles, with order $(6 \times N_v) \times (6 \times N_v)$, can be written

$$\mathbf{K}_{vv} = \mathrm{diag}[\,\mathbf{K}_{v1}\ \mathbf{K}_{v2}\ \cdots\ \mathbf{K}_{vN_v}\,] \tag{10}$$

where $\mathbf{K}_{vj}$ with order 6×6 denotes the stiffness matrix of the jth vehicle and can be expressed as

$$\mathbf{K}_{vj} = \begin{bmatrix} 2k_s & -k_sL_1 + k_sL_2 & -k_s & 0 & -k_s & 0 \\ & k_sL_1^2 + k_sL_2^2 & k_sL_1 & 0 & -k_sL_2 & 0 \\ & & k_s + 2k_p & 0 & 0 & 0 \\ & & & 2k_pL_t^2 & 0 & 0 \\ & \text{symm.} & & & k_s + 2k_p & 0 \\ & & & & & 2k_pL_t^2 \end{bmatrix} \tag{11}$$

in which L_1 denotes the horizontal distance between the centers of gravity of the car body and the ear bogie, L_2 the horizontal distance between the centers of gravity of the car body and the front bogie, and L_t half of the bogie axle base.

The damping matrix $\mathbf{C}_{vv}$ of the vehicles, with order $(6 \times N_v) \times (6 \times N_v)$, can be obtained by simply replacing k in the corresponding stiffness matrix $\mathbf{K}_{vv}$ by c.

3.3 Matrices for the rail

The matrices for the rail are marked with the subscript ‘rr’. The mass matrix $\mathbf{M}_{rr}$ of the rail, with order $N_r \times N_r$, can be written

$$\mathbf{M}_{rr} = \mathbf{M}_{rr1} + \mathbf{M}_{rr2} \tag{12}$$

with

$$\mathbf{M}_{rr2} = \sum_{j=1}^{N_v} \sum_{h=1}^{4} m_w \cdot \mathbf{N}_{jh}^{\mathrm{T}} \cdot \mathbf{N}_{jh}$$

$$\begin{aligned} \mathbf{N}_{jh} &= [\,0\ 0\ \cdots\ 0\ N_1\ N_2\ N_3\ N_4\ 0\ \cdots\ 0\ 0\,]_{\xi=\xi_{jh}} \\ N_1 &= 1 - 3(\xi/l)^2 + 2(\xi/l)^3 \quad N_2 = \xi[1 - 2(\xi/l) + (\xi/l)^2] \\ N_3 &= 3(\xi/l)^2 - 2(\xi/l)^3 \quad N_4 = \xi[(\xi/l)^2 - (\xi/l)] \end{aligned}$$

where $\mathbf{M}_{rr1}$, with order $N_r \times N_r$, represents the overall mass matrix of the rail itself, obtained by assembling all its element mass matrix $\int_0^l \bar{m}_r \mathbf{N}^{\mathrm{T}} \mathbf{N} d\xi$ with order 4×4, in which $\bar{m}_r$ denotes the rail mass per unit length, and $\mathbf{N} = [\,N_1\ N_2\ N_3\ N_4\,]$; $\mathbf{M}_{rr2}$ (with order $N_r \times N_r$) represents the overall mass matrix induced by all the wheel masses; ξ denotes the local coordinate measured from the left node of a beam element; as shown in Fig. 2, the solid circles (•) in the rail and bridge denote the nodes for the rail and bridge elements; ξ_{j1}, ξ_{j2}, ξ_{j3} and ξ_{j4} denote, respectively, the distance between the rear wheelset of rear bogie of the jth vehicle and the left node of the rail element on which the wheelset is acting, the distance between the front wheelset of rear bogie of the jth vehicle and the left node of the rail element on which the wheelset is acting, the distance between the rear wheelset of front bogie of the jth vehicle and the left node of the rail element on which the wheelset is acting, and the distance between the front wheelset of front bogie of the jth vehicle and the left node of the rail element on which the wheelset is acting; and $\mathbf{N}_{jh}$ with order $1 \times N_\mathrm{r}$ are the shape function matrices for the rail element, evaluated at the position of the hth wheelset of the jth vehicle. It should be noted that each element is zero in $\mathbf{N}_{jh}$ except those corresponding to the four DOFs of the two nodes of the rail element on which the hth wheelset of the jth vehicle is acting. $\mathbf{N}_{jh}$ is time dependent as the hth wheelset of the jth vehicle moves from one position to another within one rail element. As the hth wheelset of the jth vehicle moves to the next rail element, $\mathbf{N}_{jh}$ will shift in position corresponding to the DOFs of the rail element where the hth wheelset of the jth vehicle is positioned.

The stiffness matrix for the rail $\mathbf{K}_\mathrm{rr}$, with order $N_\mathrm{r} \times N_\mathrm{r}$, can be expressed as

$$\mathbf{K}_\mathrm{rr} = \mathbf{K}_\mathrm{rr1} + \mathbf{K}_\mathrm{rr2} + \mathbf{K}_\mathrm{rr3} \tag{13}$$

with

$$\mathbf{K}_\mathrm{rr2} = \sum_{j=1}^{N_\mathrm{v}} \sum_{h=1}^{4} [k_\mathrm{p} \cdot \mathbf{N}_{jh}^\mathrm{T} \cdot \mathbf{N}_{jh} + (c_\mathrm{p} v + m_\mathrm{w} a) \cdot \mathbf{N}_{jh}^\mathrm{T} \cdot \mathbf{N}'_{jh} + m_\mathrm{w} v^2 \cdot \mathbf{N}_{jh}^\mathrm{T} \cdot \mathbf{N}''_{jh}]$$

where $\mathbf{K}_\mathrm{rr1}$ with order $N_\mathrm{r} \times N_\mathrm{r}$ represents the overall stiffness matrix of the rail itself, obtained by assembling all its element stiffness matrix $\int_0^l E_\mathrm{r} I_\mathrm{r} \mathbf{N}''^\mathrm{T} \mathbf{N}'' d\xi$ with order 4×4, in which E_r denotes the Young's modulus of the rail, I_r denotes the constant moment of inertia of the rail cross section, and the prime denotes differentiation with respect to the local coordinate ξ; $\mathbf{K}_\mathrm{rr2}$ with order $N_\mathrm{r} \times N_\mathrm{r}$ represents the overall stiffness matrix induced by all the vehicles; $\mathbf{K}_\mathrm{rr3}$ with order $N_\mathrm{r} \times N_\mathrm{r}$ represents the overall stiffness matrix induced by the stiffness of the rail bed, obtained by assembling all the element stiffness matrix $\int_0^l k_\mathrm{rb} \mathbf{N}^\mathrm{T} \mathbf{N} d\xi$ with order 4×4 due to the rail bed supporting the rail element.

Similarly, the damping matrix of the rail, $\mathbf{C}_\mathrm{rr}$, with order $N_\mathrm{r} \times N_\mathrm{r}$, can be written

$$\mathbf{C}_\mathrm{rr} = \mathbf{C}_\mathrm{rr1} + \mathbf{C}_\mathrm{rr2} \tag{14}$$

with

$$\mathbf{C}_\mathrm{rr1} = \sum_{j=1}^{N_\mathrm{v}} \sum_{h=1}^{4} (c_\mathrm{p} \cdot \mathbf{N}_{jh}^\mathrm{T} \cdot \mathbf{N}_{jh} + 2 m_\mathrm{w} v \cdot \mathbf{N}_{jh}^\mathrm{T} \cdot \mathbf{N}'_{jh})$$

where $\mathbf{C}_\mathrm{rr1}$ with order $N_\mathrm{r} \times N_\mathrm{r}$ represents the overall damping matrix induced by all the vehicles; $\mathbf{C}_\mathrm{rr2}$ with order $N_\mathrm{r} \times N_\mathrm{r}$ represents the overall damping matrix induced by damping of rail bed, obtained by assembling all the element damping matrix $\int_0^l c_\mathrm{rb} \mathbf{N}^\mathrm{T} \mathbf{N} d\xi$ with order 4×4 due to the rail bed, supporting the rail element.

3.4 Matrices of the bridge

The matrices for the bridges are marked with the subscript "b". The mass matrix of bridges $\mathbf{M}_\mathrm{bb}$ with order $\bar{N}_\mathrm{b} \times \bar{N}_\mathrm{b}$ can be written

$$\mathbf{M}_\mathrm{bb} = \mathrm{diag}[\, \mathbf{M}_\mathrm{b1} \ \mathbf{M}_\mathrm{b2} \cdots \mathbf{M}_{\mathrm{b}N_\mathrm{b}} \,] \tag{15}$$

where $\mathbf{M}_{\mathrm{b}i}$ $(i = 1, 2, \ldots, N_\mathrm{b})$ denotes the mass matrix of the ith multi-span bridge. $\mathbf{M}_{\mathrm{b}i}$ for the ith bridge, with order $n_{\mathrm{b}i} \times n_{\mathrm{b}i}$, can be obtained by assembling all its element mass matrix $\int_0^l \bar{m}_\mathrm{b} \mathbf{N}^\mathrm{T} \mathbf{N} d\xi$ with order 4×4, in which $\bar{m}_\mathrm{b}$ denotes the bridge mass per unit length.

The stiffness matrix of the bridges $\mathbf{K}_\mathrm{bb}$, with order $\bar{N}_\mathrm{b} \times \bar{N}_\mathrm{b}$, can be written

$$\mathbf{K}_\mathrm{bb} = \mathrm{diag}[\, \mathbf{K}_\mathrm{b1} \ \mathbf{K}_\mathrm{b2} \cdots \mathbf{K}_{\mathrm{b}N_\mathrm{b}} \,] \tag{16}$$

where $\mathbf{K}_{\mathrm{b}i}$ $(i = 1, 2, \ldots, N_\mathrm{b})$ denotes the stiffness matrix of the ith multi-span bridge. $\mathbf{K}_{\mathrm{b}i}$ of the ith bridge with order $n_{\mathrm{b}i} \times n_{\mathrm{b}i}$ can be expressed as

$$\mathbf{K}_{\mathrm{b}i} = \mathbf{K}_{\mathrm{b}i1} + \mathbf{K}_{\mathrm{b}i2} \tag{17}$$

where $\mathbf{K}_{\mathrm{b}i1}$ with order $n_{\mathrm{b}i} \times n_{\mathrm{b}i}$ represents the overall stiffness matrix of the ith bridge itself, obtained by assembling all its element stiffness matrix $\int_0^l E_\mathrm{b} I_\mathrm{b} \mathbf{N}''^\mathrm{T} \mathbf{N}'' d\xi$ with order 4×4, in which E_b denotes the Young's modulus of the bridge, and I_b the constant moment of inertia of the bridge cross section; $\mathbf{K}_{\mathrm{b}i2}$ with order $n_{\mathrm{b}i} \times n_{\mathrm{b}i}$ represents the overall stiffness matrix induced by the stiffness of the rail bed, obtained by assembling all the element stiffness matrix $\int_0^l k_\mathrm{rb} \mathbf{N}^\mathrm{T} \mathbf{N} d\xi$ with order 4×4 due to the rail bed connecting the bridge element.

Similarly, the damping matrix of the bridges $\mathbf{C}_\mathrm{bb}$ with order $\bar{N}_\mathrm{b} \times \bar{N}_\mathrm{b}$ can be written

$$\mathbf{C}_\mathrm{bb} = \mathrm{diag}[\,\mathbf{C}_{\mathrm{b}1}\ \mathbf{C}_{\mathrm{b}2}\ \cdots\ \mathbf{C}_{\mathrm{b}N_\mathrm{b}}\,] \tag{18}$$

where $\mathbf{C}_{\mathrm{b}i}$ ($i = 1, 2, \ldots, N_\mathrm{b}$) denotes the damping matrix of the ith multi-span bridge. $\mathbf{C}_{\mathrm{b}i}$ for the ith bridge, with order $n_{\mathrm{b}i} \times n_{\mathrm{b}i}$, can be expressed as

$$\mathbf{C}_{\mathrm{b}i} = \mathbf{C}_{\mathrm{b}i1} + \mathbf{C}_{\mathrm{b}i2} \tag{19}$$

in which $\mathbf{C}_{\mathrm{b}i1}$ with order $n_{\mathrm{b}i} \times n_{\mathrm{b}i}$ represents the overall damping matrix of the ith bridge, and $\mathbf{C}_{\mathrm{b}i2}$ with order $n_{\mathrm{b}i} \times n_{\mathrm{b}i}$ represents the overall damping matrix induced by the damping of the rail bed, obtained by assembling all the element damping matrix $\int_0^l c_\mathrm{rb} \mathbf{N}^\mathrm{T} \mathbf{N} d\xi$ of order 4×4 due to the rail bed connecting the bridge element.

On the basis of the definition of Rayleigh damping, the damping matrix $\mathbf{C}_{\mathrm{b}i1}$ of the ith bridge, with order $n_{\mathrm{b}i} \times n_{\mathrm{b}i}$, is computed as follows:

$$\mathbf{C}_{\mathrm{b}i1} = \alpha \cdot \mathbf{M}_{\mathrm{b}i} + \beta \cdot \mathbf{K}_{\mathrm{b}i1} \tag{20}$$

Given the damping ratio ζ_b, the two coefficients α and β can be determined as $\alpha = 2\zeta_\mathrm{b}\omega_1\omega_2/(\omega_1 + \omega_2)$, $\beta = 2\zeta_\mathrm{b}/(\omega_1 + \omega_2)$, where ω_1 and ω_2 are the first two natural circular frequencies of vibration of the bridge [2,26].

3.5 Matrices of the vehicles–rail interaction

The matrices induced by the vehicles–rail interaction are denoted by the subscript 'vr' or 'rv'. The stiffness matrices $\mathbf{K}_\mathrm{vr}$ with order $(6 \times N_\mathrm{v}) \times N_\mathrm{r}$ and $\mathbf{K}_\mathrm{rv}$ with order $N_\mathrm{r} \times (6 \times N_\mathrm{v})$, the damping matrices $\mathbf{C}_\mathrm{vr}$ with order $(6 \times N_\mathrm{v}) \times N_\mathrm{r}$ and $\mathbf{C}_\mathrm{rv}$ with order $N_\mathrm{r} \times (6 \times N_\mathrm{v})$ induced by the interaction between the vehicles and the rail can be written as

$$\mathbf{K}_\mathrm{vr} = \sum_{j=1}^{N_\mathrm{v}} \mathbf{K}_{\mathrm{v}_j\mathrm{r}_1} + \sum_{j=1}^{N_\mathrm{v}} \mathbf{K}_{\mathrm{v}_j\mathrm{r}_2} + \sum_{j=1}^{N_\mathrm{v}} \mathbf{K}_{\mathrm{v}_j\mathrm{r}_3} + \sum_{j=1}^{N_\mathrm{v}} \mathbf{K}_{\mathrm{v}_j\mathrm{r}_4} \tag{21}$$

$$\mathbf{K}_\mathrm{rv} = \sum_{j=1}^{N_\mathrm{v}} \mathbf{K}_{\mathrm{r}_1\mathrm{v}_j} + \sum_{j=1}^{N_\mathrm{v}} \mathbf{K}_{\mathrm{r}_2\mathrm{v}_j} + \sum_{j=1}^{N_\mathrm{v}} \mathbf{K}_{\mathrm{r}_3\mathrm{v}_j} + \sum_{j=1}^{N_\mathrm{v}} \mathbf{K}_{\mathrm{r}_4\mathrm{v}_j} \tag{22}$$

$$\mathbf{C}_\mathrm{vr} = \sum_{j=1}^{N_\mathrm{v}} \mathbf{C}_{\mathrm{v}_j\mathrm{r}_1} + \sum_{j=1}^{N_\mathrm{v}} \mathbf{C}_{\mathrm{v}_j\mathrm{r}_2} + \sum_{j=1}^{N_\mathrm{v}} \mathbf{C}_{\mathrm{v}_j\mathrm{r}_3} + \sum_{j=1}^{N_\mathrm{v}} \mathbf{C}_{\mathrm{v}_j\mathrm{r}_4} \tag{23}$$

$$\mathbf{C}_\mathrm{rv} = \sum_{j=1}^{N_\mathrm{v}} \mathbf{C}_{\mathrm{r}_1\mathrm{v}_j} + \sum_{j=1}^{N_\mathrm{v}} \mathbf{C}_{r_2\mathrm{v}_j} + \sum_{j=1}^{N_\mathrm{v}} \mathbf{C}_{\mathrm{r}_3\mathrm{v}_j} + \sum_{j=1}^{N_\mathrm{v}} \mathbf{C}_{\mathrm{r}_4\mathrm{v}_j} \tag{24}$$

with

$$\mathbf{K}_{\mathrm{v}_j\mathrm{r}_1} = \begin{bmatrix} \mathbf{0} \\ \mathbf{0} \\ \vdots \\ -k_\mathrm{p}\mathbf{N}_{j1} - c_\mathrm{p} v \mathbf{N}'_{j1} \\ k_\mathrm{p} L_\mathrm{t} \mathbf{N}_{j1} + c_\mathrm{p} L_\mathrm{t} v \mathbf{N}'_{j1} \\ \vdots \\ \mathbf{0} \\ \mathbf{0} \end{bmatrix}_{(6\times N_\mathrm{v})\times N_\mathrm{r}} \qquad \mathbf{K}_{\mathrm{v}_j\mathrm{r}_2} = \begin{bmatrix} \mathbf{0} \\ \mathbf{0} \\ \vdots \\ -k_\mathrm{p}\mathbf{N}_{j2} - c_\mathrm{p} v \mathbf{N}'_{j2} \\ -k_\mathrm{p} L_\mathrm{t} \mathbf{N}_{j2} - c_\mathrm{p} L_\mathrm{t} v \mathbf{N}'_{j2} \\ \vdots \\ \mathbf{0} \\ \mathbf{0} \end{bmatrix}_{(6\times N_\mathrm{v})\times N_\mathrm{r}}$$

$$\mathbf{K}_{\mathrm{v}_j\mathrm{r}_3} = \begin{bmatrix} \mathbf{0} \\ \mathbf{0} \\ \vdots \\ -k_\mathrm{p}\mathbf{N}_{j3} - c_\mathrm{p}v\mathbf{N}'_{j3} \\ k_\mathrm{p}L_\mathrm{t}\mathbf{N}_{j3} + c_\mathrm{p}L_\mathrm{t}v\mathbf{N}'_{j3} \\ \vdots \\ \mathbf{0} \\ \mathbf{0} \end{bmatrix}_{(6\times N_\mathrm{v})\times N_\mathrm{r}} \qquad \mathbf{K}_{\mathrm{v}_j\mathrm{r}_4} = \begin{bmatrix} \mathbf{0} \\ \mathbf{0} \\ \vdots \\ -k_\mathrm{p}\mathbf{N}_{j4} - c_\mathrm{p}v\mathbf{N}'_{j4} \\ -k_\mathrm{p}L_\mathrm{t}\mathbf{N}_{j4} - c_\mathrm{p}L_\mathrm{t}v\mathbf{N}'_{j4} \\ \vdots \\ \mathbf{0} \\ \mathbf{0} \end{bmatrix}_{(6\times N_\mathrm{v})\times N_\mathrm{r}}$$

$$\begin{aligned}
\mathbf{K}_{\mathrm{r}_1\mathrm{v}_j} &= [\mathbf{0}\ \mathbf{0}\ \ldots\ -k_\mathrm{p}\mathbf{N}_{j1}^\mathrm{T}\ k_\mathrm{p}L_\mathrm{t}\mathbf{N}_{j1}^\mathrm{T}\ \ldots\ \mathbf{0}\ \mathbf{0}]_{N_\mathrm{r}\times(6\times N_\mathrm{v})} \\
\mathbf{K}_{\mathrm{r}_2\mathrm{v}_j} &= [\mathbf{0}\ \mathbf{0}\ \ldots\ -k_\mathrm{p}\mathbf{N}_{j2}^\mathrm{T}\ -k_\mathrm{p}L_\mathrm{t}\mathbf{N}_{j2}^\mathrm{T}\ \ldots\ \mathbf{0}\ \mathbf{0}]_{N_\mathrm{r}\times(6\times N_\mathrm{v})} \\
\mathbf{K}_{\mathrm{r}_3\mathrm{v}_j} &= [\mathbf{0}\ \mathbf{0}\ \ldots\ -k_\mathrm{p}\mathbf{N}_{j3}^\mathrm{T}\ k_\mathrm{p}L_\mathrm{t}\mathbf{N}_{j3}^\mathrm{T}\ \ldots\ \mathbf{0}\ \mathbf{0}]_{N_\mathrm{r}\times(6\times N_\mathrm{v})} \\
\mathbf{K}_{\mathrm{r}_4\mathrm{v}_j} &= [\mathbf{0}\ \mathbf{0}\ \ldots\ -k_\mathrm{p}\mathbf{N}_{j4}^\mathrm{T}\ -k_\mathrm{p}L_\mathrm{t}\mathbf{N}_{j4}^\mathrm{T}\ \ldots\ \mathbf{0}\ \mathbf{0}]_{N_\mathrm{r}\times(6\times N_\mathrm{v})}
\end{aligned}$$

$$\mathbf{C}_{\mathrm{v}_j\mathrm{r}_1} = \mathbf{C}_{\mathrm{r}_1\mathrm{v}_j}^\mathrm{T} = \begin{bmatrix} \mathbf{0} \\ \mathbf{0} \\ \vdots \\ -c_\mathrm{p}\mathbf{N}_{j1} \\ c_\mathrm{p}L_\mathrm{t}\mathbf{N}_{j1} \\ \vdots \\ \mathbf{0} \\ \mathbf{0} \end{bmatrix}_{(6\times N_\mathrm{v})\times N_\mathrm{r}} \qquad \mathbf{C}_{\mathrm{v}_j\mathrm{r}_2} = \mathbf{C}_{\mathrm{r}_2\mathrm{v}_j}^\mathrm{T} = \begin{bmatrix} \mathbf{0} \\ \mathbf{0} \\ \vdots \\ -c_\mathrm{p}\mathbf{N}_{j2} \\ -c_\mathrm{p}L_\mathrm{t}\mathbf{N}_{j2} \\ \vdots \\ \mathbf{0} \\ \mathbf{0} \end{bmatrix}_{(6\times N_\mathrm{v})\times N_\mathrm{r}}$$

$$\mathbf{C}_{\mathrm{v}_j\mathrm{r}_3} = \mathbf{C}_{\mathrm{r}_3\mathrm{v}_j}^\mathrm{T} = \begin{bmatrix} \mathbf{0} \\ \mathbf{0} \\ \vdots \\ -c_\mathrm{p}\mathbf{N}_{j3} \\ c_\mathrm{p}L_\mathrm{t}\mathbf{N}_{j3} \\ \vdots \\ \mathbf{0} \\ \mathbf{0} \end{bmatrix}_{(6\times N_\mathrm{v})\times N_\mathrm{r}} \qquad \mathbf{C}_{\mathrm{v}_j\mathrm{r}_4} = \mathbf{C}_{\mathrm{r}_4\mathrm{v}_j}^{T} = \begin{bmatrix} \mathbf{0} \\ \mathbf{0} \\ \vdots \\ -c_\mathrm{p}\mathbf{N}_{j4} \\ -c_\mathrm{p}L_\mathrm{t}\mathbf{N}_{j4} \\ \vdots \\ \mathbf{0} \\ \mathbf{0} \end{bmatrix}_{(6\times N_\mathrm{v})\times N_\mathrm{r}}$$

where $\mathbf{K}_{\mathrm{v}_j\mathrm{r}_1}$ and $\mathbf{K}_{\mathrm{r}_1\mathrm{v}_j}$ represent the stiffness matrices induced by the interaction between the rear wheelset of the rear bogie of the jth vehicle and the rail, and $\mathbf{C}_{\mathrm{v}_j\mathrm{r}_1}$ and $\mathbf{C}_{\mathrm{r}_1\mathrm{v}_j}$ are the corresponding damping matrices; $\mathbf{K}_{\mathrm{v}_j\mathrm{r}_2}$ and $\mathbf{K}_{\mathrm{r}_2\mathrm{v}_j}$ represent the stiffness matrices induced by the interaction between the front wheelset of rear bogie of the jth vehicle and the rail, and $\mathbf{C}_{\mathrm{v}_j\mathrm{r}_2}$ and $\mathbf{C}_{\mathrm{r}_2\mathrm{v}_j}$ are the corresponding damping matrices; $\mathbf{K}_{\mathrm{v}_j\mathrm{r}_3}$ and $\mathbf{K}_{\mathrm{r}_3\mathrm{v}_j}$ represent the stiffness matrices induced by the interaction between the rear wheelset of the front bogie of the jth vehicle and the rail, and $\mathbf{C}_{\mathrm{v}_j\mathrm{r}_3}$ and $\mathbf{C}_{\mathrm{r}_3\mathrm{v}_j}$ the corresponding damping matrices; $\mathbf{K}_{\mathrm{v}_j\mathrm{r}_4}$ and $\mathbf{K}_{\mathrm{r}_4\mathrm{v}_j}$ represent the stiffness matrices induced by the interaction between the front wheelset of front bogie of the jth vehicle and the rail, and $\mathbf{C}_{\mathrm{v}_j\mathrm{r}_4}$ and $\mathbf{C}_{\mathrm{r}_4\mathrm{v}_j}$ the corresponding damping matrices. It should be noted that each row is a zero vector in $\mathbf{K}_{\mathrm{v}_j\mathrm{r}_1}$, $\mathbf{K}_{\mathrm{v}_j\mathrm{r}_2}$, $\mathbf{C}_{\mathrm{v}_j\mathrm{r}_1}$ and $\mathbf{C}_{\mathrm{v}_j\mathrm{r}_2}$ except those that correspond to the two DOFs of the rear bogie frame of the jth vehicle, and each column is a zero vector in $\mathbf{K}_{\mathrm{r}_1\mathrm{v}_j}$, $\mathbf{K}_{\mathrm{r}_2\mathrm{v}_j}$, $\mathbf{C}_{\mathrm{r}_1\mathrm{v}_j}$ and $\mathbf{C}_{\mathrm{r}_2\mathrm{v}_j}$ except those that correspond to the two DOFs of the rear bogie frame of the jth vehicle; each row is a zero vector in $\mathbf{K}_{\mathrm{v}_j\mathrm{r}_3}$, $\mathbf{K}_{\mathrm{v}_j\mathrm{r}_4}$, $\mathbf{C}_{\mathrm{v}_j\mathrm{r}_3}$ and $\mathbf{C}_{\mathrm{v}_j\mathrm{r}_4}$ except those corresponding to the two DOFs of the front bogie frame of the jth vehicle, and each column is a zero vector in $\mathbf{K}_{\mathrm{r}_3\mathrm{v}_j}$, $\mathbf{K}_{\mathrm{r}_4\mathrm{v}_j}$, $\mathbf{C}_{\mathrm{r}_3\mathrm{v}_j}$ and $\mathbf{C}_{\mathrm{r}_4\mathrm{v}_j}$ except those corresponding to the two DOFs of the front bogie frame of the jth vehicle.

3.6 Matrices of the rail–bridge interaction

The matrices induced by the continuous springs and dampers between the rail and bridges are denoted by the subscripts 'rb' or 'br'. The stiffness matrix $\mathbf{K}_\mathrm{br}$ with order $\bar{N}_\mathrm{b} \times N_\mathrm{r}$ induced by the continuous springs between the rail and bridges can be written as

$$\mathbf{K}_{\mathrm{br}} = [\, \mathbf{K}_{\mathrm{br_L}} \; \mathbf{K}_{\mathrm{br_C}} \; \mathbf{K}_{\mathrm{br_R}} \,] \tag{25}$$

where $\mathbf{K}_{\mathrm{br_L}}$ with order $\bar{N}_{\mathrm{b}} \times N_{\mathrm{r_L}}$ denotes the stiffness matrix induced by the continuous springs between the bridges and the rail in the left track segment, $N_{\mathrm{r_L}}$ denotes the number of DOFs of the rail in the left track segment except the DOFs of the rail node A (as shown in Fig. 1); $\mathbf{K}_{\mathrm{br_R}}$ with order $\bar{N}_{\mathrm{b}} \times N_{\mathrm{r_R}}$ denotes the stiffness matrix induced by the continuous springs between the bridges and the rail in the right track segment, $N_{\mathrm{r_R}}$ denotes the number of DOFs of the rail in the right track segment except the DOFs of the rail node B (as shown in Fig. 1); $\mathbf{K}_{\mathrm{br_C}}$ with order $\bar{N}_{\mathrm{b}} \times N_{\mathrm{r_C}}$ denotes the stiffness matrix induced by the continuous springs between the bridges and the rail in the central track segment, N_{r_C} denotes the number of DOFs of the rail in the central track segment including the DOFs of the rail nodes A and B. It should be noted that $N_{\mathrm{r}} = N_{\mathrm{r}_L} + N_{\mathrm{r}_C} + N_{\mathrm{r_R}}$, and that each element in $\mathbf{K}_{\mathrm{br_L}}$ and $\mathbf{K}_{\mathrm{br_R}}$ is zero.

$\mathbf{K}_{\mathrm{br_C}}$ consists of the stiffness matrices $\mathbf{K}_{\mathrm{b_1 r_{C1}}}$ with order $n_{\mathrm{b}1} \times n_{\mathrm{b}1}$, $\mathbf{K}_{\mathrm{b_2 r_{C2}}}$ with order $n_{\mathrm{b}2} \times n_{\mathrm{b}2}, \ldots, \mathbf{K}_{\mathrm{b_{N_b} r_{CN_b}}}$ with order $n_{\mathrm{b}N_{\mathrm{b}}} \times n_{\mathrm{b}N_{\mathrm{b}}}$, and is zero in other positions, where $\mathbf{K}_{\mathrm{b}_i \mathrm{r}_{\mathrm{C}i}}$ $(i = 1, 2, \ldots, N_{\mathrm{b}})$ with order $n_{\mathrm{b}i} \times n_{\mathrm{b}i}$ denotes the stiffness matrix induced by the continuous springs between the ith multi-span bridge and the rail supported on the ith multi-span bridge, and $\mathbf{K}_{\mathrm{b}_i \mathrm{r}_{\mathrm{C}i}}$ with order $n_{\mathrm{b}i} \times n_{\mathrm{b}i}$ can be obtained by assembling all the stiffness matrix $-\int_0^l k_{\mathrm{rb}} \mathbf{N}^{\mathrm{T}} \mathbf{N} d\xi$ with order 4×4 induced by the continuous springs between the bridge element and the corresponding rail element of the ith multi-span bridge. $\mathbf{K}_{\mathrm{b}_i \mathrm{r}_{\mathrm{C}i}}$ $(i = 1, 2, \ldots, N_{\mathrm{b}})$ should be the position from the $\left(\sum_{s=1}^{i-1} n_{\mathrm{b}s}\right)$th row and the $(\sum_{s=1}^{i-1} n_{\mathrm{b}s} - 2 \times (i-1))$th column to the $(\sum_{s=1}^{i} n_{\mathrm{b}s})$th row and the $(\sum_{s=1}^{i} n_{\mathrm{b}s} - 2 \times (i-1))$th column in the stiffness matrix $\mathbf{K}_{\mathrm{br_C}}$ if $i > 1$, and from the first row and the first column to the $n_{\mathrm{b}1}$th row and the $n_{\mathrm{b}1}$th column in the stiffness matrix $\mathbf{K}_{\mathrm{br_C}}$ if $i = 1$.

It should be noted that $\mathbf{K}_{\mathrm{rb}} = \mathbf{K}_{\mathrm{br}}^{\mathrm{T}}$.

The damping matrices $\mathbf{C}_{\mathrm{br}}$ with order $\bar{N}_{\mathrm{b}} \times N_{\mathrm{r}}$ and $\mathbf{C}_{\mathrm{rb}}$ with order $N_{\mathrm{r}} \times \bar{N}_{\mathrm{b}}$ induced by the continuous dampers between the rail and bridges can be obtained by simply replacing k in the corresponding stiffness matrices $\mathbf{K}_{\mathrm{br}}$ and $\mathbf{K}_{\mathrm{rb}}$ by c, respectively.

3.7 Load vectors of vehicles, rail and bridge

The load vector $\mathbf{F}_{\mathrm{v}}$ of vehicles, with order $(6 \times N_{\mathrm{v}}) \times 1$, can be written

$$\mathbf{F}_{\mathrm{v}} = [\, \mathbf{F}_{\mathrm{v}1} \; \mathbf{F}_{\mathrm{v}2} \cdots \mathbf{F}_{\mathrm{v}N_{\mathrm{v}}} \,]^{\mathrm{T}} \tag{26}$$

where $\mathbf{F}_{\mathrm{v}j}$ with order 6×1 is the load vector of the jth vehicle

$$\mathbf{F}_{\mathrm{v}j} = \begin{Bmatrix} 0 \\ 0 \\ k_{\mathrm{p}} r_{\xi=\xi_{j1}} + k_{\mathrm{p}} r_{\xi=\xi_{j2}} + c_{\mathrm{p}} v r'_{\xi=\xi_{j1}} + c_{\mathrm{p}} v r'_{\xi=\xi_{j2}} \\ -k_{\mathrm{p}} L_{\mathrm{t}} r_{\xi=\xi_{j1}} + k_{\mathrm{p}} L_{\mathrm{t}} r_{\xi=\xi_{j2}} - c_{\mathrm{p}} v L_{\mathrm{t}} r'_{\xi=\xi_{j1}} + c_{\mathrm{p}} v L_{\mathrm{t}} r'_{\xi=\xi_{j2}} \\ k_{\mathrm{p}} r_{\xi=\xi_{j3}} + k_{\mathrm{p}} r_{\xi=\xi_{j4}} + c_{\mathrm{p}} v r'_{\xi=\xi_{j3}} + c_{\mathrm{p}} v r'_{\xi=\xi_{j4}} \\ -k_{\mathrm{p}} L_{\mathrm{t}} r_{\xi=\xi_{j3}} + k_{\mathrm{p}} L_{\mathrm{t}} r_{\xi=\xi_{j4}} - c_{\mathrm{p}} v L_{\mathrm{t}} r'_{\xi=\xi_{j3}} + c_{\mathrm{p}} v L_{\mathrm{t}} r'_{\xi=\xi_{j4}} \end{Bmatrix} \tag{27}$$

The load vector $\mathbf{F}_{\mathrm{r}}$ with order $N_{\mathrm{r}} \times 1$ of rail can be written as

$$\mathbf{F}_{\mathrm{r}} = \sum_{j=1}^{N_{\mathrm{v}}} \mathbf{F}_{\mathrm{r}j1} + \sum_{j=1}^{N_{\mathrm{v}}} \mathbf{F}_{\mathrm{r}j2} + \sum_{j=1}^{N_{\mathrm{v}}} \mathbf{F}_{\mathrm{r}j3} + \sum_{j=1}^{N_{\mathrm{v}}} \mathbf{F}_{\mathrm{r}j4} \tag{28}$$

with

$$\mathbf{F}_{\mathrm{r}j1}=\left(m_{\mathrm{w}}g+\frac{1}{2}m_{\mathrm{t}}g+\frac{1}{2}m_{\mathrm{c}}g\frac{L_2}{L_1+L_2}-k_{\mathrm{p}}\cdot r_{\xi=\xi_{j1}}-c_{\mathrm{p}}v\cdot r'_{\xi=\xi_{j1}}-m_{\mathrm{w}}a\cdot r'_{\xi=\xi_{j1}}-m_{\mathrm{w}}v^2\cdot r''_{\xi=\xi_{j1}}\right)\mathbf{N}_{j1}^{\mathrm{T}}$$

$$\mathbf{F}_{\mathrm{r}j2}=\left(m_{\mathrm{w}}g+\frac{1}{2}m_{\mathrm{t}}g+\frac{1}{2}m_{\mathrm{c}}g\frac{L_2}{L_1+L_2}-k_{\mathrm{p}}\cdot r_{\xi=\xi_{j2}}-c_{\mathrm{p}}v\cdot r'_{\xi=\xi_{j2}}-m_{\mathrm{w}}a\cdot r'_{\xi=\xi_{j2}}-m_{\mathrm{w}}v^2\cdot r''_{\xi=\xi_{j2}}\right)\mathbf{N}_{j2}^{\mathrm{T}}$$

$$\mathbf{F}_{\mathrm{r}j3}=\left(m_{\mathrm{w}}g+\frac{1}{2}m_{\mathrm{t}}g+\frac{1}{2}m_{\mathrm{c}}g\frac{L_1}{L_1+L_2}-k_{\mathrm{p}}\cdot r_{\xi=\xi_{j3}}-c_{\mathrm{p}}v\cdot r'_{\xi=\xi_{j3}}-m_{\mathrm{w}}a\cdot r'_{\xi=\xi_{j3}}-m_{\mathrm{w}}v^2\cdot r''_{\xi=\xi_{j3}}\right)\mathbf{N}_{j3}^{\mathrm{T}}$$

$$\mathbf{F}_{\mathrm{r}j4}=\left(m_{\mathrm{w}}g+\frac{1}{2}m_{\mathrm{t}}g+\frac{1}{2}m_{\mathrm{c}}g\frac{L_1}{L_1+L_2}-k_{p}\cdot r_{\xi=\xi_{j4}}-c_{p}v\cdot r'_{\xi=\xi_{j4}}-m_{\mathrm{w}}a\cdot r'_{\xi=\xi_{j4}}-m_{\mathrm{w}}v^2\cdot r''_{\xi=\xi_{j4}}\right)\mathbf{N}_{j4}^{T}$$

where $\mathbf{F}_{\mathrm{r}j1}$, $\mathbf{F}_{\mathrm{r}j2}$, $\mathbf{F}_{\mathrm{r}j3}$ and $\mathbf{F}_{\mathrm{r}j4}$ represent the load vectors induced by the rear wheelset of rear bogie, the front wheelset of rear bogie, the rear wheelset of front bogie, and the front wheelset of front bogie of the jth vehicle acting on the rail, respectively.

All elements in the load vector of the bridges $\mathbf{F}_{\mathrm{b}}$, with order $\bar{N}_{\mathrm{b}} \times 1$, are zero.

Since $\mathbf{N}_{jh}$ ($j = 1, 2, \ldots, N_{\mathrm{v}}$, and $h = 1, \ldots, 4$), $r_{\xi=\xi_{jh}}$, and their differentiation with respect to the local coordinate ξ are time dependent. Therefore, the matrices and the load vectors containing $\mathbf{N}_{jh}$, $r_{\xi=\xi_{jh}}$, and their differentiation, i.e., the matrices $\mathbf{M}_{\mathrm{rr}}$, $\mathbf{C}_{\mathrm{vr}}$, $\mathbf{C}_{\mathrm{rv}}$, $\mathbf{C}_{\mathrm{rr}}$, $\mathbf{K}_{\mathrm{vr}}$, $\mathbf{K}_{\mathrm{rv}}$, and $\mathbf{K}_{\mathrm{rr}}$, and the load vectors $\mathbf{F}_{\mathrm{v}}$ and $\mathbf{F}_{\mathrm{r}}$ in Eq. (1) are also time dependent. They must be updated at each time step.

Equation (1) can be solved by the step-by-step integration method such as the Newmark-β method [21] or Wilson-θ method [3], to obtain simultaneously the dynamic responses of train, of track and of bridges. Equation (1) has been written on the assumption that N_{v} vehicles are acting on the track concerned. If a certain vehicles is not on the track concerned, the corresponding rows and columns of the matrix equation should be deleted.

Equation (1) can be applied not only to the analysis of the dynamic responses of the interaction system among a moving train or single vehicle, a railway track and several types of railway bridges, such as a multi-span or a series of multi-span railway bridges and a single-span or a series of single-span simply supported bridges, but also to the analysis of the dynamic responses of a beam on viscoelastic foundation, a single-span simply supported beam or a multi-span continuous beam subjected to a moving train.

4 Verification of the proposed procedure

In this section, the equation of motion derived for the train–track–bridge interaction system and the associated computer program will be verified through the study of an example. Let us consider a simply supported Bernoulli–Euler bridge with a smooth top surface and ignored track subjected to a moving train consisting of five identical four-wheelset vehicles with constant speeds from 10 to 110 m/s with increments of 1 m/s. All parameters of the vehicle and bridge are listed in Table 1. The first natural circular frequency for the bridge computed is $\omega_1 = 25.62$ rad/s.

To make use of the proposed procedure, the following data are assumed for the track: $L_{\mathrm{r}} = 32$ m, $E_{\mathrm{r}} = 2.943 \times 10^{10}$ Pa, $I_{\mathrm{r}} = 2.88\,\mathrm{m}^4$, $\bar{m}_{\mathrm{r}} = 1.2 \times 10^4$ kg/m, $k_{\mathrm{rb}} = 0\,\mathrm{N/m}^2$, and $c_{\mathrm{rb}} = 0\,\mathrm{Ns/m}^2$. That is to say, the parameters of track are the same as those of the aforementioned bridge. It should be pointed out that the proposed computer program has considered the damping of rail itself by using similar Eq. (20). In generally, ζ_{r} (the damping ratio of rail) is zero, i.e., the damping of rail is neglected, in analysis of the dynamic responses of the train–track–bridge system. However, ζ_{r} is equal to 0.02 in this example. The following data are assumed for bridge: $L = 32$ m, $E_{\mathrm{b}} = 2.943 \times 10^{10}$ Pa (arbitrary nonzero value), $I_{\mathrm{b}} = 2.88\,\mathrm{m}^4$ (arbitrary nonzero value), $\bar{m}_{\mathrm{b}} = 1.2 \times 10^4$ kg/m (arbitrary nonzero value), $\zeta_{\mathrm{b}} = 0.02$ (arbitrary value), and $N_{\mathrm{b}} = 1$. Because both k_{rb} and c_{rb} are zero, in the present results, the dynamic responses of rail obtained by the proposed procedure are those of the aforementioned bridge.

In the present analysis, both rail and bridge are divided into 10 elements of equal length. It is assumed that the rail and bridge is at rest at the instant of train arrival. The equation of motion for this system is solved by the Wilson-θ method with $\theta = 1.4$. Figures 3 and 4, respectively, show the dynamic magnification factors for vertical displacement and bending moment at the midpoint of the rail against train speed obtained by the

Table 1 All parameters for the vehicle and bridge

Notation	Parameter	Value
	Vehicle	
m_c	Mass of the car body	4.175×10^4 kg
J_c	Mass moment of inertia of the car body	2.08×10^6 kg m^2
L_d	Horizontal distance between the center of the rear bogie of a four-wheelset vehicle and the center of the front bogie of the following four-wheelset vehicle	6.0 m
k_s	Spring stiffness of the second suspension system	5.3×10^5 N/m
c_s	Damping coefficient of the second suspension system	9.02×10^4 N s/m
L_1	Horizontal distance between the centers of gravity of the car body and the rear bogie	8.75 m
L_2	Horizontal distance between the centers of gravity of the car body and the front bogie	8.75 m
m_t	Mass of a bogie frame	3.04×10^3 kg
J_t	Mass moment of inertia of a bogie frame	3.93×10^3 kg m^2
L_t	Half of the bogie axle base	1.25 m
k_p	Spring stiffness of the primary suspension system	1.18×10^6 N/m
c_p	Damping coefficient of the primary suspension system	3.92×10^4 Ns/m
m_w	Mass of a wheelset	1.78×10^3 kg
	Bridge	
E_b	Young's modulus	2.943×10^{10} Pa
I_b	Moment of inertia	2.88 m^4
$\bar{m}_b$	Mass per unit length	1.2×10^4 kg/m
L	Span length	32 m
ζ_b	Damping ratio	0.02

proposed procedure using 2,000 equal time steps for each train speed, along with the results obtained by Lou et al. [18] using the modal analysis method (MAM) considering the first five modes of the bridge. The dynamic magnification factors for vertical displacement and bending moment at a specified section are defined as:

Dynamic magnification factor for vertical displacement = (maximum dynamic vertical displacement)/(maximum static vertical displacement)

Dynamic magnification factor for bending moment = (maximum dynamic bending moment)/(maximum static bending moment)

From Figs. 3 and 4, one observes that good agreement has been achieved between the present and MAM solutions. There is slight deviation in Fig. 4. The reason is that the beam deflection converges faster than the beam bending moment in the MAM. The example serves to illustrate the reliability of the proposed procedure.

In addition, as can be seen from Figs. 3 and 4, there are a few local peak values at various speeds, indicating the occurrence of a train–bridge resonance at that speed. The reason can be given as follows. From Yang et al. [30], it is known that the dimensionless resonant speed parameter is $S_{\text{res}} = d/(2nL)$, where d is the vehicle length, L is the bridge span length, and n is a positive integer. Furthermore, from Yang et al. [27], the speed parameter S is taken as $S = v\pi/(\omega_1 L)$. When $d = 23.5$ m, $L = 32$ m, and $\omega_1 = 25.62$ rad/s, one can obtain the resonance speed as $v_{\text{res}} = 95.82/n$ (m/s). On the other hand, from Yang et al. [30], it is also known that the dimensionless speed parameter for the waves generated by the moving axles loads to cancel each other is $S_{\text{can}} = 1/(2\bar{n}-1)$, where $\bar{n}$ is a positive integer. Equivalently, the cancelation speed is $v_{\text{can}} = 260.96/(2\bar{n}-1)$. As shown in Figs. 3 and 4, the resonant speeds with $v_{\text{res}} = 96$ and 32 m/s can be observed, while the other resonant speeds are suppressed since they are coincident with or close to the point of cancelation.

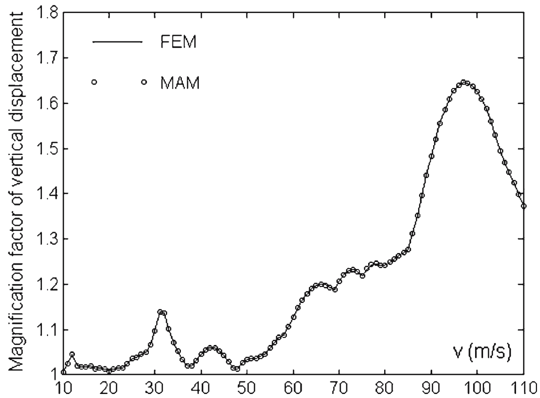

Fig. 3 Dynamic magnification factor for the vertical displacement of the bridge midpoint under various train speeds

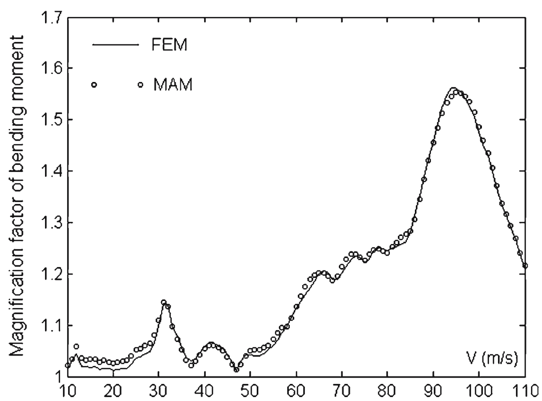

Fig. 4 Dynamic magnification factor for the bending moment of the bridge midpoint under various train speeds

5 Numerical examples

In the following examples, the effect of two types of vehicle models, two types of bridge models and three damping values of bridge on the maximum dynamic responses of train, track and bridges will be investigated. The equation of motion for the train–track–bridge interaction system is also solved by the Wilson-θ method with $\theta = 1.4$. The running speed of the train is constant from 10 to 200 m/s with increment of 2 m/s. For the case of each speed, 2,000 equal time steps are used to analyze the dynamic responses of this system. It should be noted that the calculated accelerations for vehicle, rail and bridge in the following examples are absolute value.

5.1 Example 1: The effect of two types of vehicle models on the dynamic responses of the train–track–bridge interaction system

The effect of two types of vehicle models on the dynamic responses of the train–track–bridge interaction system is investigated in this section. As an illustration example, let us consider a three-span continuous beam to model the bridge with the track structure under a moving train using two types of vehicle models. One is a four-wheelset whole-vehicle model, that is, each vehicle is considered as a four-wheelset mass–spring–damper system, as shown in Fig. 2; the other is a half-vehicle model, that is, each four-wheelset vehicle is considered as two two-wheelset mass–spring–damper system, as shown in Fig. 5. The train consists of five identical four-wheelset vehicles with two-stage suspensions. A railway track is continuous throughout a three-span continuous beam with the two approaches supported on embankments. The parameters of the vehicle and bridge are the same as those in Table 1 except L. In this example, L (the span length) is 30 m, and the total length of the three-span continuous beam is 90 m. The parameters of track concerned with top smooth surface are listed in Table 2. It is assumed that the length of track structure on each approach embankment is equal,

Table 2 The parameters for the track

Notation	Parameter	Value
L_r	Total length of the track structure concerned	138 m
E_r	Young's modulus	2.06×10^{11} Pa
I_r	Moment of inertia	$2\times2.037\times10^{-5}$ m^4
$\bar{m}_r$	Mass per unit length	2×51.5 kg/m
k_{rb}	Stiffness of the continuous springs reflecting the properties of the rail bed	$2\times6.58\times10^7$ N/m^2
c_{rb}	Damping coefficient of the continuous dampers reflecting the properties of the rail bed	$2\times3.21\times10^4$ N s/m^2

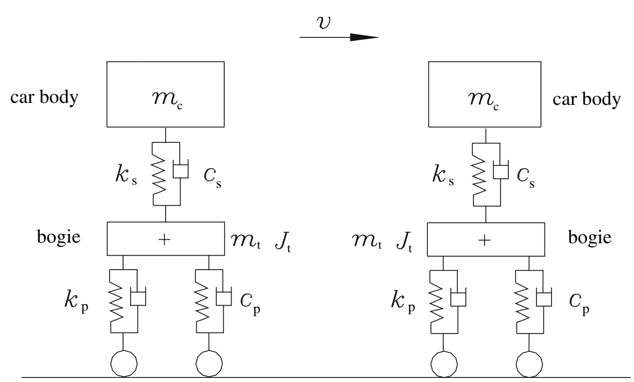

Fig. 5 Two half-vehicle models

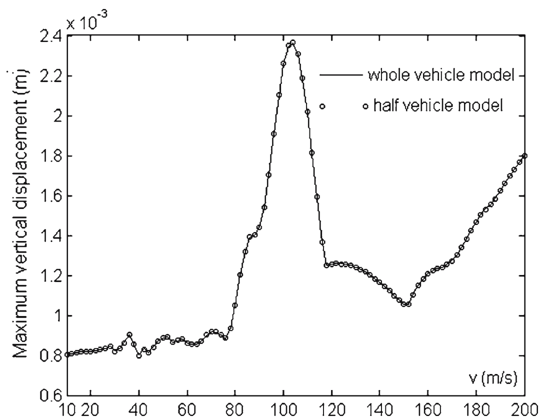

Fig. 6 Maximum vertical displacement at the midpoint of the bridge for the two types of vehicle models

i.e., the length of the left track segment equals to that of the right track segment. The first two frequencies for the bridge computed by the solution of eigenvalue for the bridge free vibration or by [8] are $\omega_1 = 29.145$ rad/s and $\omega_2 = 37.215$ rad/s, respectively. In the finite element analysis, the three-span continuous beam is divided into 60 elements each of length 1.5 m, and the rails is divided into 92 elements each of length 1.5 m. For the half-vehicle model, all the parameters of the vehicle, the track and the bridge are the same as those in this example except $m_c = 0.5 \times 4.175 \times 10^4$ kg and $J_c = 0$ kg·m^2. For the two types of vehicle models, the maximum dynamic responses of train, track and bridge under various train speed have been plotted in Figs. 6, 7, 8, 9, 10, 11, 12 and 13.

From Figs. 6, 7, 8, 9, 10, 11, one observes that the effects of the two types of vehicle models on the dynamic response of rail and bridge are insignificant. However, from Figs. 12, and 13, the effect of the two types of vehicle models on the vertical acceleration of the car body is significant. The omission of the interaction between the front and rear bogies of the four-wheelset vehicle, as implied by the half-vehicle model, may result in significant underestimation of the vehicle response, which is not conservative from the design point of view.

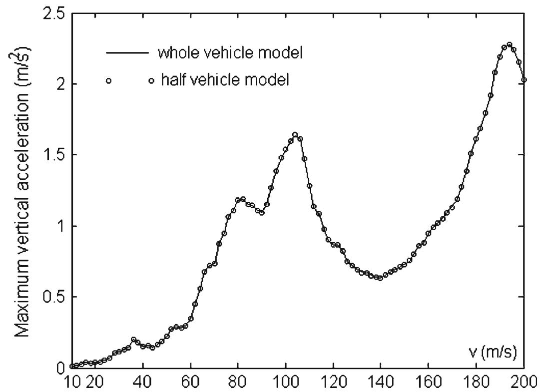

Fig. 7 Maximum vertical acceleration at the midpoint of the bridge for the two types of vehicle models

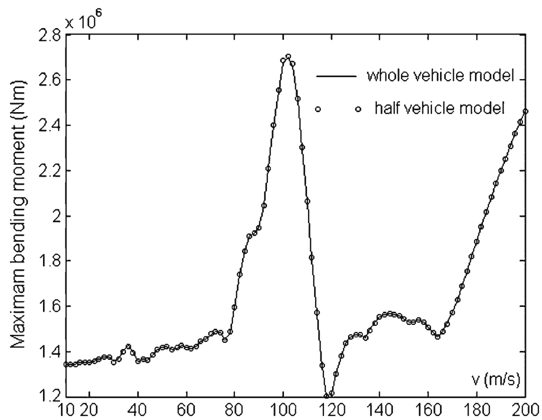

Fig. 8 Maximum bending moment at the midpoint cross section of the bridge for the two types of vehicle models

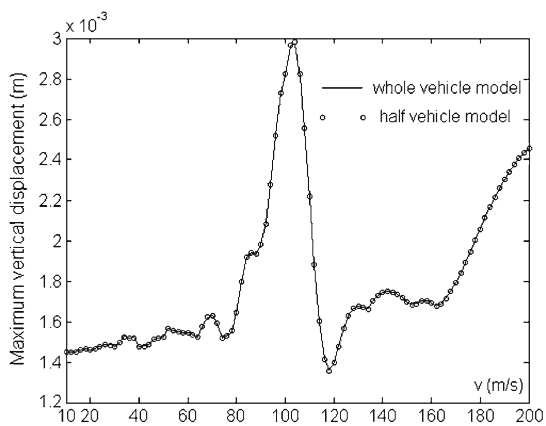

Fig. 9 Maximum vertical displacement at the midpoint of the rail for the two types of vehicle models

5.2 Example 2: The effect of two types of bridge models on the dynamic responses of the train–track–bridge interaction system

In order to analyze the effect of different bridge models on the dynamic responses of the train–track–bridge interaction system, let us consider two types of bridge models: one is the model of a three-span continuous beam to model bridge and the other is the model of three single-span simple beams to model bridges. In this study, the whole-vehicle model mentioned in Example 1 is used. All the parameters of the train, the track and the bridge are the same as those in Example 1. For the two types of bridge models, the maximum dynamic

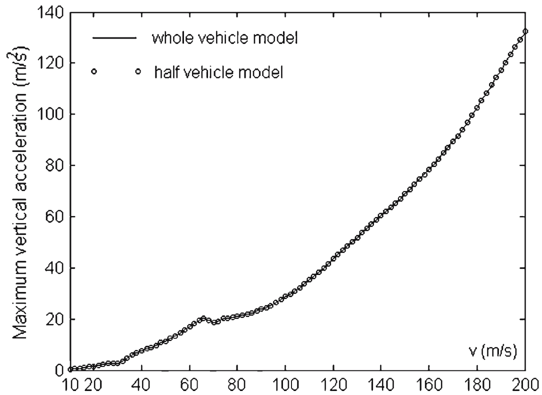

Fig. 10 Maximum vertical acceleration at the midpoint of the rail for the two types of vehicle models

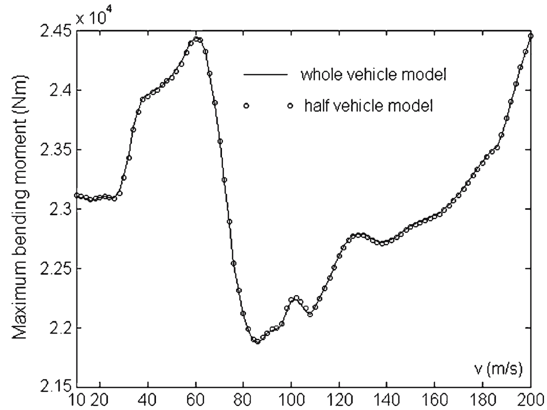

Fig. 11 Maximum bending moment at the midpoint cross section of the rail for the two types of vehicle models

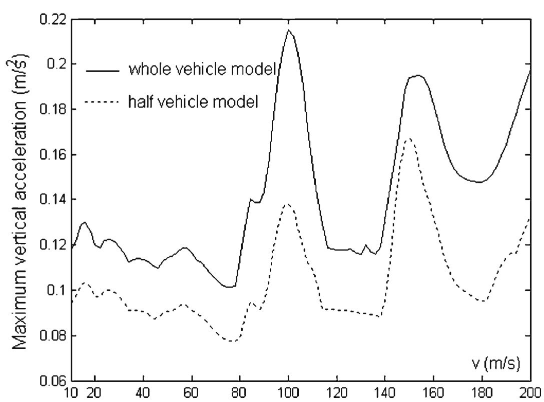

Fig. 12 Maximum vertical acceleration at the last car body above the center of gravity of the rear bogie for the two types of vehicle models

responses of train, track and bridge under various train speed have been plotted in Figs. 14, 15, 16, 17, 18, 19 and 20.

As can be seen from Fig. 14, 15, 16, 17, 19 and 20 the displacement, acceleration and bending moment of bridge, the displacement and bending moment of rail and the vertical acceleration of the car body for the continuous beam model are smaller than those for the simple beam model. Therefore, in the bridge design, the continuous beam may be adopted to reduce the dynamic response of the bridge, the displacement of the rail and the acceleration of the car body. However, from Fig. 18, one observes that the effect of the bridge model on the vertical acceleration of the rail is insignificant.

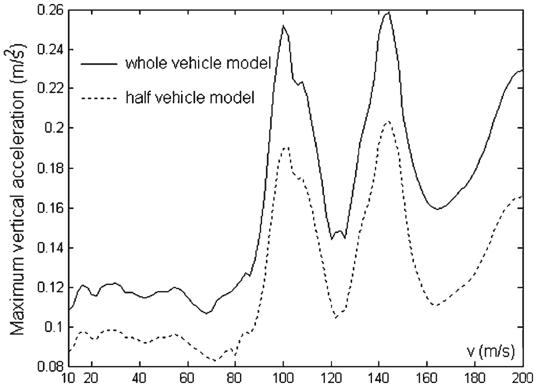

Fig. 13 Maximum vertical acceleration at the last car body above the center of gravity of the front bogie for the two types of vehicle models

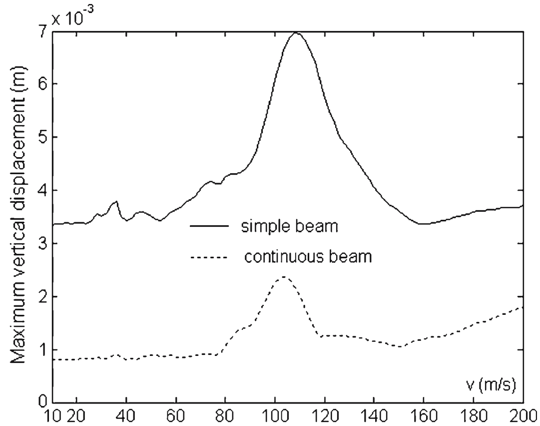

Fig. 14 Maximum vertical displacement at the midpoint of the central span of the bridge for the two types of bridge models

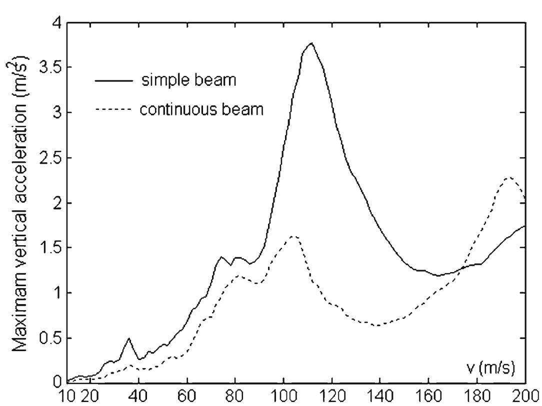

Fig. 15 Maximum vertical acceleration at the midpoint of the central span of the bridge for the two types of bridge models

5.3 Example 3: The effect of different damping values of the bridge on the dynamic responses of the train–track–bridge interaction system

The effect of three types of damping ratios of bridge, such as $\zeta = 0$, $\zeta = 0.02$ and $\zeta = 0.04$, on the dynamic responses of the train–track–bridge interaction system is studied in this section. In this study, the whole-vehicle model mentioned in Example 1 is used. All the parameters of the train, the track and the bridge are the same as in Example 1 except for the damping ratio of bridge. For the three types of damping ratios of bridge,

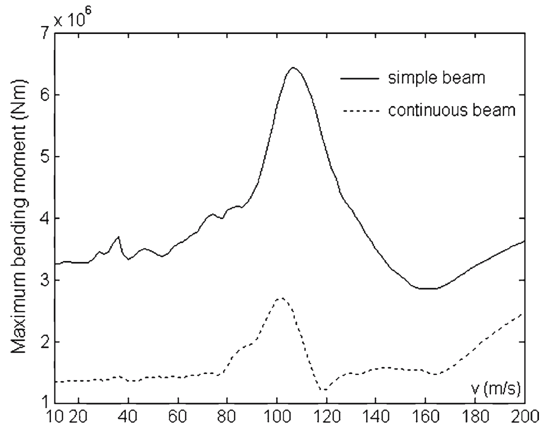

Fig. 16 Maximum bending moment at the midpoint cross section of the central span of the bridge for the two types of bridge models

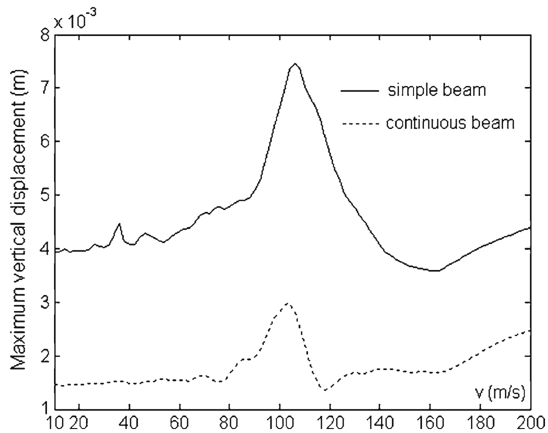

Fig. 17 Maximum vertical displacement at the midpoint of the rail for the two types of bridge models

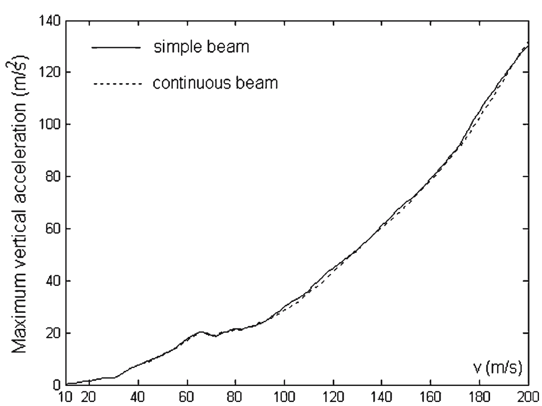

Fig. 18 Maximum vertical acceleration at the midpoint of the rail for the two types of bridge models

the maximum dynamic responses of train, track and bridge under various train speed have been plotted in Figs. 21, 22, 23, 24, 25, 26 and 27.

As shown in Figs. 21, 22, 23, 24 and 27, the amplitudes at resonance for the displacement, acceleration and bending moment of bridge, the displacement of the rail and the vertical acceleration of the car body decrease very quickly as the damping ratio of the bridge increases. Therefore, the increase of damping for the bridge is an effective measure to reduce the resonant amplitudes for the train–track–bridge interaction system. As can

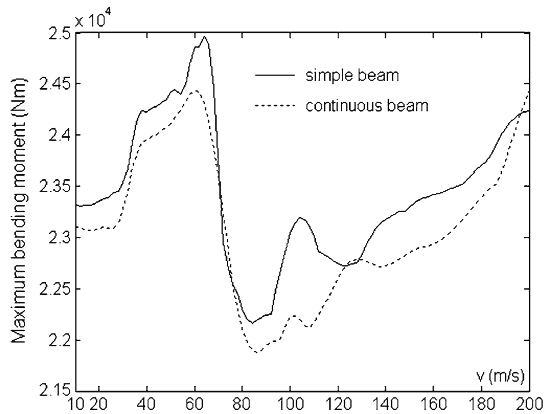

Fig. 19 Maximum bending moment at the midpoint cross section of the rail for the two types of bridge models

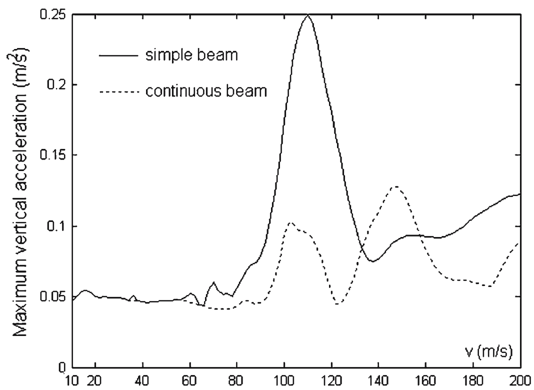

Fig. 20 Maximum vertical acceleration at the center of gravity of the last car body for the two types of bridge models

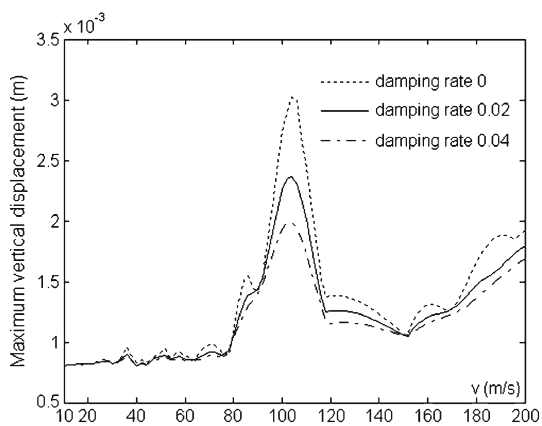

Fig. 21 Maximum vertical displacement at the midpoint of the bridge for the different bridge damping ratios

be seen from Figs. 25 and 26, however, the effect of the damping ratio of bridge on the vertical acceleration and bending moment of the rail is insignificant.

6 Concluding remarks

On the basis of the finite element method, the equation of motion for the train–track–bridge interaction system in matrix form with time-dependent coefficients is presented. Using the present equation, the dynamic

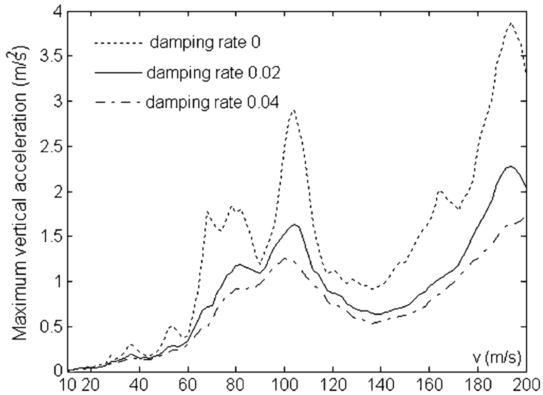

Fig. 22 Maximum vertical acceleration at the midpoint of the bridge for the different bridge damping ratios

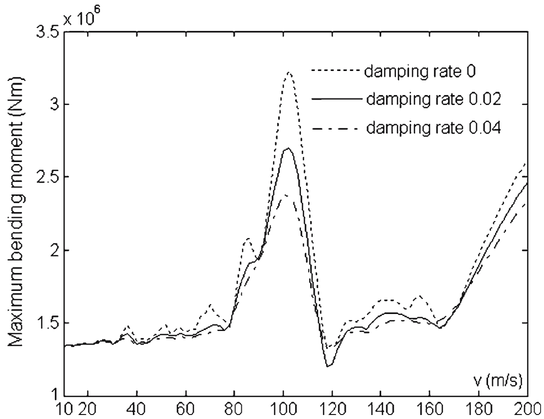

Fig. 23 Maximum bending moment at the midpoint cross section of the bridge for the different bridge damping ratios

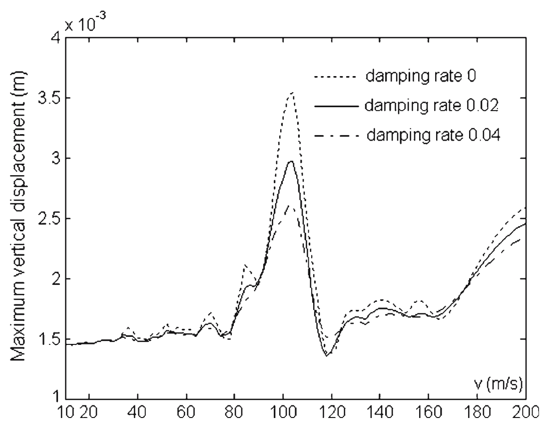

Fig. 24 Maximum vertical displacement at the midpoint of the rail for the different bridge damping ratios

responses of the interaction system among a moving train or single vehicle, the railway track and several types of railway bridge, including a multi-span or a series of identical multi-span continuous beams to model railway bridges and a single-span or a series of identical single-span simple beams to model railway bridges, can be analyzed. In addition, the dynamic responses of a beam on a viscoelastic foundation or a single-span simple beam subjected to a moving train can also be analyzed by using the presented equation. The effect of two types of vehicle models, two types of bridge models and three types damping ratio of bridge on the maximum dynamic responses of train, track and bridges are investigated. From the investigation, several conclusions can be drawn:

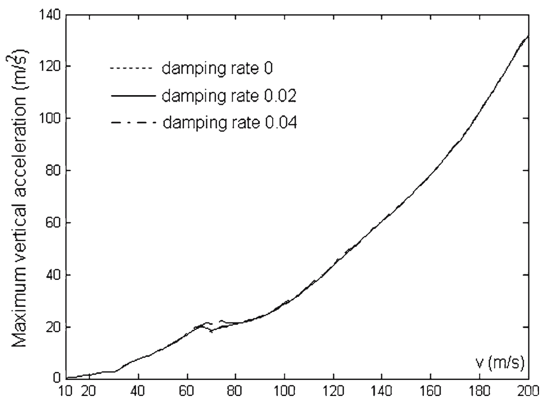

Fig. 25 Maximum vertical acceleration at the midpoint of the rail for the different bridge damping ratios

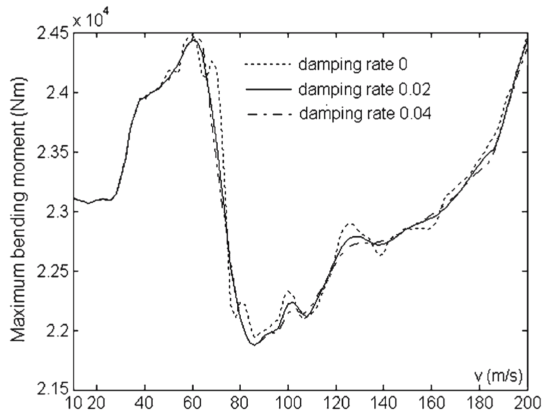

Fig. 26 Maximum bending moment at the midpoint cross section of the rail for the different bridge damping ratios

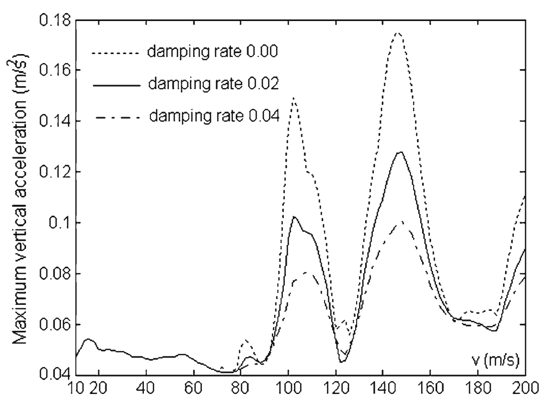

Fig. 27 Maximum vertical acceleration at the gravity center of the last car body for the different bridge damping ratios

1. The effects of the whole-vehicle model and the half-vehicle model on the dynamic responses of the rail and bridge are insignificant; however, they have a significant effect on the the vertical acceleration of the car body. The omission of the interaction between the front and rear bogies of the four-wheelset vehicle, as implied by the half-vehicle model, may result in a significant underestimation of the vehicle response, which is not conservative from the design point of view.
2. The displacement, acceleration and bending moment of the bridge, the displacement and bending moment of the rail and the vertical acceleration of the car body using the continuous beam model are smaller than those using the simple beam model. Therefore, in the design of a bridge, the continuous beam model may

be adopted to reduce the dynamic responses of the bridge, the displacement of the rail and the acceleration of the car body. However, the effect of bridge models on the vertical acceleration of the rail is insignificant.

3. The resonant amplitudes for the displacement, acceleration and bending moment of the bridge, the displacement of the rail and the vertical acceleration of the car body decrease very quickly as the damping ratio of the bridge increases. Thus, increasing the damping of the bridge is an effective measure to reduce the resonant amplitudes for the train–track–bridge interaction system. However, the effect of the damping ratio of the bridge on the vertical acceleration and bending moment of the rail is insignificant.

Acknowledgment The author would like to thank Prof. Reinhold Kienzler, Editor-in-Chief, Archive of Applied Mechanics, and two anonymous reviewers for their valuable and helpful comments.

References

1. Au, F.T.K., Cheng, Y.S., Cheung, Y.K.: Vibration analysis of bridges under moving vehicles and trains: an overview. Prog. Struct. Eng. Mater. **3**(3), 299–304 (2001)
2. Au, F.T.K., Wang, J.J., Cheung, Y.K.: Impact study of cable-stayed bridge under railway traffic using various models. J. Sound Vib. **240**(3), 447–465 (2001)
3. Bathe, K.J., Wilson, E.L.: Numerical Methods in Finite Element Analysis. Prentice-Hall, Englewood Cliffs(1976)
4. Chatterjee, P.K., Datta, T.K., Surana, C.S.: Vibration of continuous bridges under moving vehicles. J. Sound Vib. **169**(5), 619–632 (1994)
5. Cheng, Y.S., Au, F.T.K., Cheung, Y.K.: Vibration of railway bridges under a moving train by using bridge-track-vehicle element. Eng. Struct. **23**(12), 1597–1606 (2001)
6. Cheung, Y.K., Au, F.T.K., Zheng, D.Y., Cheng, Y.S.: Vibration of multi-span non-uniform bridges under moving vehicles and trains by using modified beam vibration functions. J. Sound Vib. **228**(3), 611–628 (1999)
7. Chu, K.H., Garg, V.K., Wang, T.L.: Impact in railway prestressed concrete bridges. J. Struct. Eng. (ASCE) **112**(5), 1036–1051 (1986)
8. Frýba, L.: Dynamics of Railway Bridges. Thomas Telford, London, pp 67–77 (1996)
9. Frýba, L.: A rough assessment of railway bridges for high speed trains. Eng. Struct. **23**(5), 548–556 (2001)
10. Henchi, K., Fafard, M., Dhatt, G., Talbot, M.: Dynamic behaviour of multi-span beams under moving loads. J. Sound Vibr. **199**(1), 33–50 (1997)
11. Ichikawa, M., Miyakawa, Y., Matsuda, A.: Vibration analysis of the continuous beam subjected to a moving mass. J. Sound Vib. **230**(3), 493–506 (2000)
12. Kortuem, W., Wormley, D.N.: Dynamic Interactions between Travelling Vehicles and Guideway Systems. Veh. Syst. Dyn. **10**((4–5), 285–317 (1981)
13. Le, R., Ripke, B., Zacher, M.: Ballast mats on high speed bridges. In: Proceedings of the Fourth European Conference on Structural Dynamics, EURODYN'99, Prague (Czech Republic), pp. 699–703 (1999)
14. Li, J., Su, M.: The resonant vibration for a simply supported girder bridge under high-speed trains. J. Sound Vib. **224**(5), 897–915 (1999)
15. Lou, P.: A vehicle-track-bridge interaction element considering vehicle's pitching effect. Finite Elem. Anal. Des. **41**(4), 397–427 (2005)
16. Lou, P.: Vertical dynamic responses of a simply supported bridge subjected to a moving train with two-wheelset vehicles using modal analysis method. Int. J. Numer. Methods Eng. **64**(9), 1207–1235 (2005)
17. Lou, P.: Comparison of two types of deflection functions for analyzing the responses of the rail and the bridge under static or moving vehicles. Proc. Inst. Mech. Eng. K J. Multibody Dyn. **220**(2), 105–123 (2006)
18. Lou, P., Dai, G.L., Zeng, Q.Y.: Modal coordinate formulations for a simply supported bridge subjected to a moving train modelled as two-stage suspension vehicles. Proc. Inst. Mech. Eng. C J. Mech. Eng. Sci. **219**(10), 1027–1040 (2005)
19. Lou, P., Zeng, Q.Y.: Formulation of equations of motion of finite element form for vehicle-track-bridge interaction system with two types of vehicle model. Int. J. Numer. Methods Eng. **62**(3), 435–474 (2005)
20. Lou, P., Zeng, Q.Y.: Finite element based formulations for vehicle–bridge interaction system considering vertical motion. J. Struct. Eng. **32**(4), 261–273 (2005)
21. Newmark, N.M.: A method of computation for structural dynamics. J. Eng. Mech. Div. (ASCE) **85**(3), 67–94 (1959)
22. Olsson, M.: Finite element, modal co-ordinate analysis of structures subjected to moving loads. J. Sound Vib. **99**(1), 1–12 (1985)
23. Paz, M.: Modified dynamic condensation method. J. Struct. Eng. (ASCE) **115**(1), 234–238 (1989)
24. Wang, T.L., Garg, V.K., Chu, K.H.: Railway bridge/vehicle interaction studies with new vehicle model. J. Struct. Eng. (ASCE) **117**(7), 2099–2116 (1991)
25. Wiriyachai, A., Chu, K.H., Garg, V.K.: Bridge impact due to wheel and track irregularities. J. Eng. Mech. (ASCE) **108**(4), 648–666 (1982)
26. Wu, Y.S., Yang, Y.B.: Steady-state response and riding comfort of trains moving over a series of simply supported bridges. Eng. Struct. **25**(2), 251–265 (2003)
27. Yang, Y.B., Chang, C.H., Yau, J.D.: An element for analyzing vehicle-bridge systems considering vehicle's pitching effect. Int. J. Numer. Methods Eng. **46**(7), 1031–1047 (1999)
28. Yang, Y.B., Lin, B.H.: Vehicle-bridge interaction analysis by dynamic condensation method. J. Struct. Eng. (ASCE) **121**(11), 1636–1643 (1995)

29. Yang, Y.B., Yau, J.D.: Vehicle-bridge interaction element for dynamic analysis. J. Struct. Eng.(ASCE) **123**(11), 1512–1518 (1997)
30. Yang, Y.B., Yau, J.D., Hsu, L.C.: Vibration of simple beams due to trains moving at high speeds. Eng. Struct. **19**(11), 936–944 (1997)
31. Yau, J.D., Yang, Y.B., Kuo, S.R.: Impact response of high speed rail bridges and riding comfort of rail cars. Eng. Struct. **21**(9), 836–844 (1999)
32. Zeng, Q.Y.: The principle of a stationary value of total potential energy of dynamic system(in Chinese). J. Huazhong Univ. Sci. Technol. **28**(1), 1–3 (2001)
33. Zeng, Q.Y., Guo, X.R.: Theory and Application of Vibration Analysis of Train-Bridge Time-Dependent System. China Railway Publishing House, Beijing, pp. 15–48 (1999)